

Semiconductor

Byungwoo Park

**Department of Materials Science and Engineering
Seoul National University**

<http://bp.snu.ac.kr>

Semiconductors

Kittel, Solid State Physics (Chapters 7 and 8).

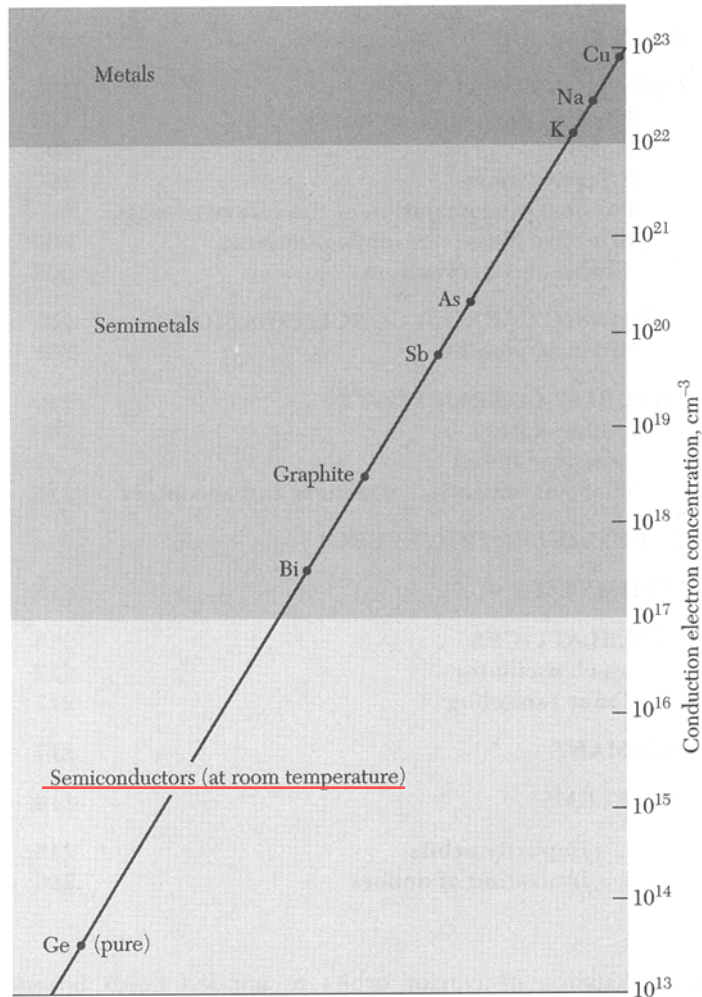
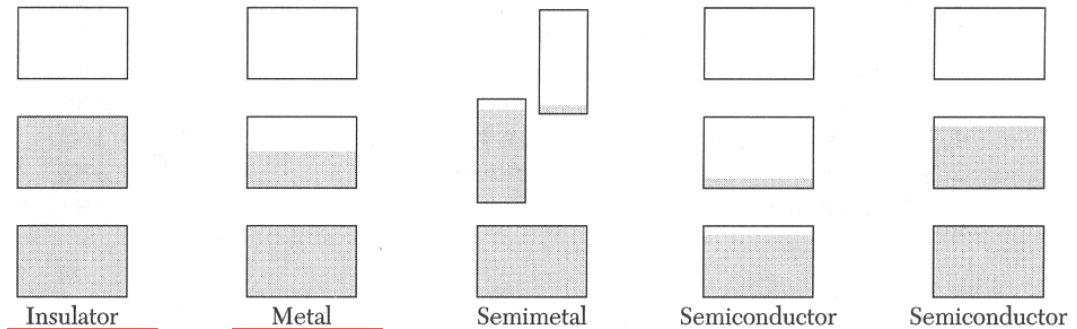


Table 1 Energy gap between the valence and conduction bands
(*i* = indirect gap; *d* = direct gap)

Crystal	Gap	E_g , eV		Crystal	Gap	E_g , eV	
		0 K	300 K			0 K	300 K
Diamond	<i>i</i>	5.4		SiC(hex)	<i>i</i>	3.0	—
Si	<i>i</i>	1.17	1.11	Tc	<i>d</i>	0.33	—
Ge	<i>i</i>	0.744	0.66	HgTe ^a	<i>d</i>	-0.30	
α Sn	<i>d</i>	0.00	0.00	PbS	<i>d</i>	0.286	0.34–0.37
InSb	<i>d</i>	0.23	0.17	PbSe	<i>i</i>	0.165	0.27
InAs	<i>d</i>	0.43	0.36	PbTe	<i>i</i>	0.190	0.29
InP	<i>d</i>	1.42	1.27	CdS	<i>d</i>	2.582	2.42
GaP	<i>i</i>	2.32	2.25	CdSe	<i>d</i>	1.840	1.74
GaAs	<i>d</i>	1.52	1.43	CdTe	<i>d</i>	1.607	1.44
GaSb	<i>d</i>	0.81	0.68	SnTe	<i>d</i>	0.3	0.18
AlSb	<i>i</i>	1.65	1.6	Cu ₂ O	<i>d</i>	2.172	—



Semiconductor Crystal

- Intrinsic semiconductor

Energy band (at 0 K)

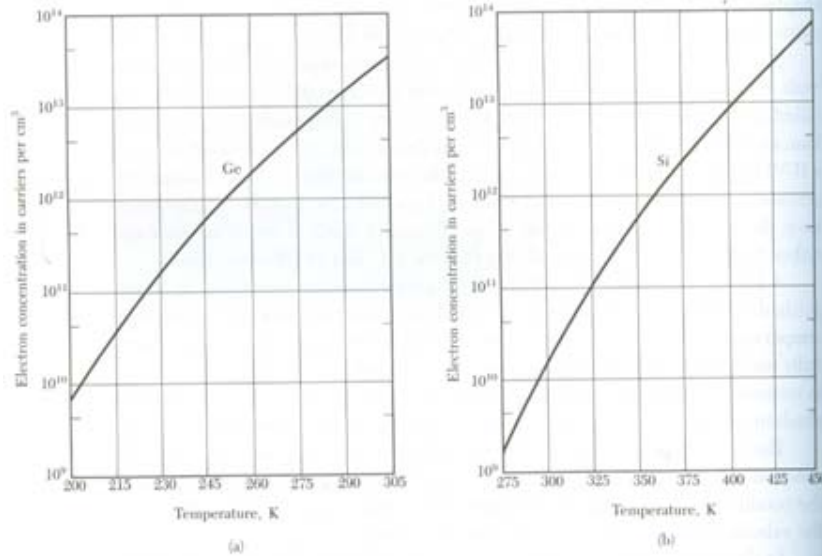
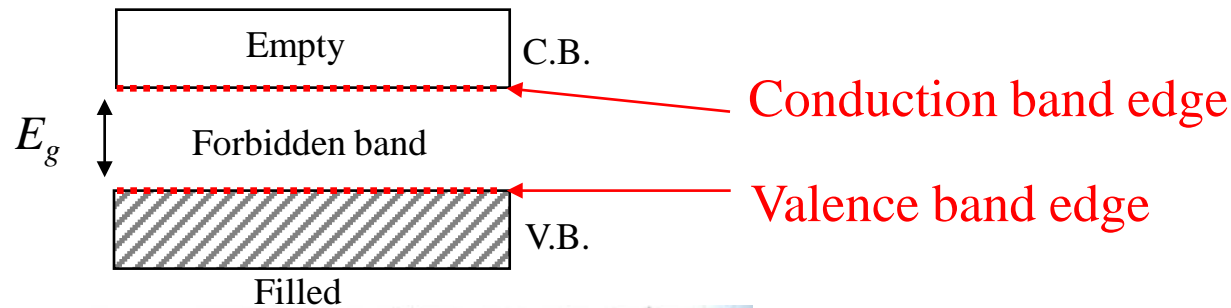


Figure 3 Intrinsic electron concentration as a function of temperature for (a) germanium and (b) silicon. Under intrinsic conditions the hole concentration is equal to the electron concentration. The intrinsic concentration at a given temperature is higher in Ge than in Si because the energy gap is narrower in Ge (0.66 eV) than in Si (1.11 eV). (After W. C. Dunlap.)

- As the temperature increases, electrons are **thermally excited** from the valence band to the conduction band.
- **Both the electrons in the conduction band and holes in valence band** contribute to the electrical conductivity.

Kittel, Solid State Physics (Chapter 8).

Energy Band of Semiconductors

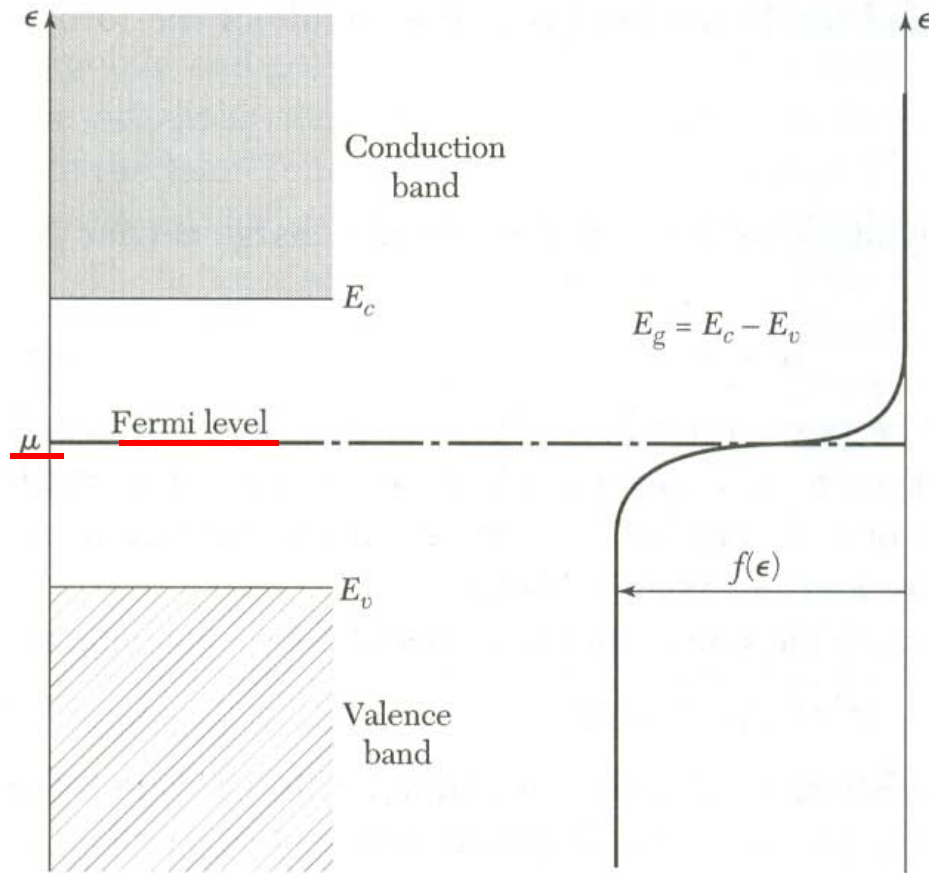
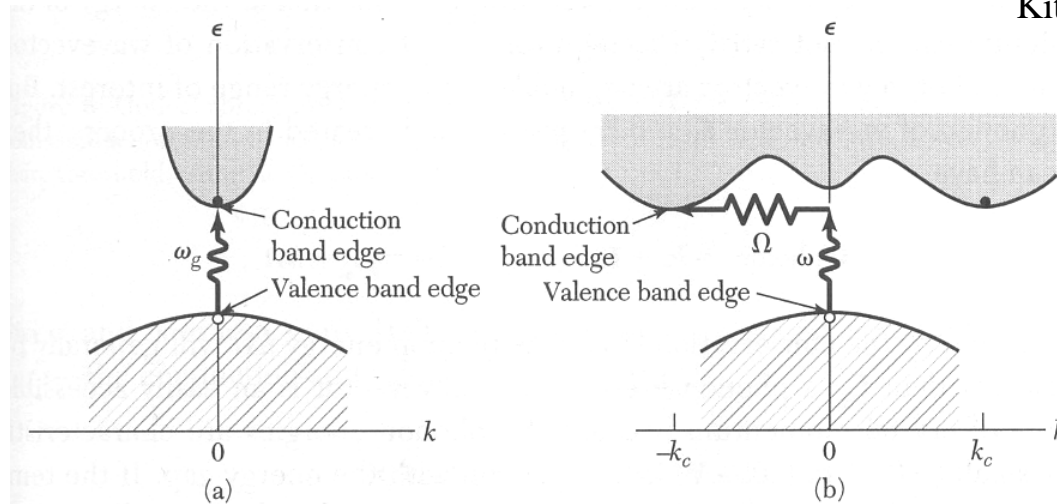


Figure 18 Energy scale for statistical calculations. The Fermi distribution function is shown on the same scale, for a temperature $k_B T \ll E_g$. The Fermi level μ is taken to lie well within the band gap, as for an intrinsic semiconductor. If $\epsilon = \mu$, then $f = \frac{1}{2}$.

Kittel, Solid State Physics (Chapter 8).

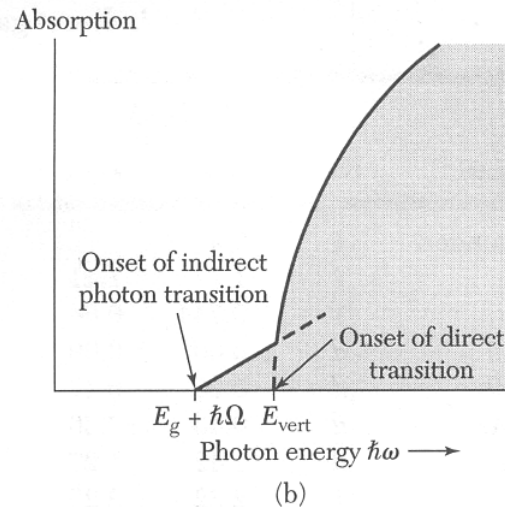
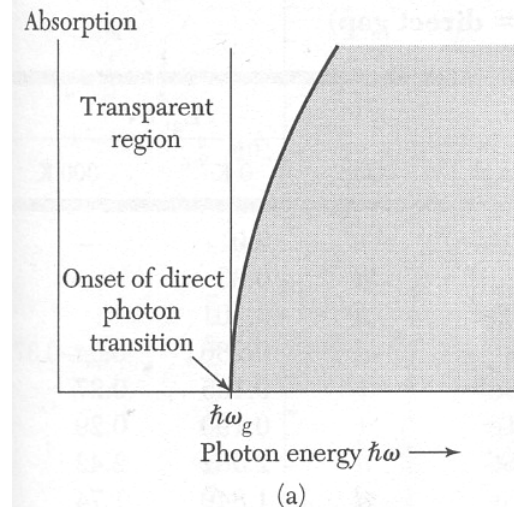
Direct Bandgap vs. Indirect Bandgap

Kittel, Solid State Physics (Chapter 8).



CRYSTAL WITH DIRECT GAP

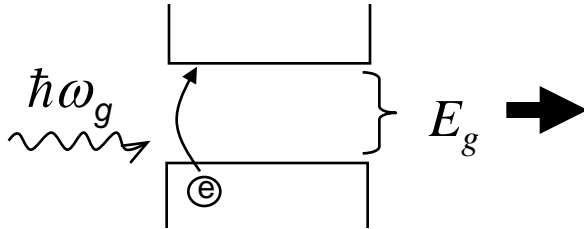
CRYSTAL WITH INDIRECT GAP



$$\mathbf{k}(\text{photon}) = \mathbf{k}_c + \mathbf{K} \cong \mathbf{0} ; \quad \hbar\omega = E_g + \hbar\Omega$$

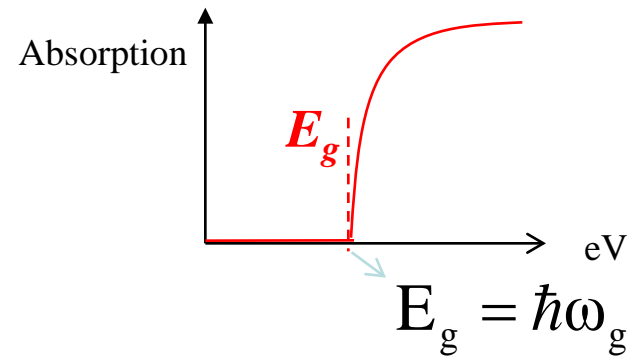
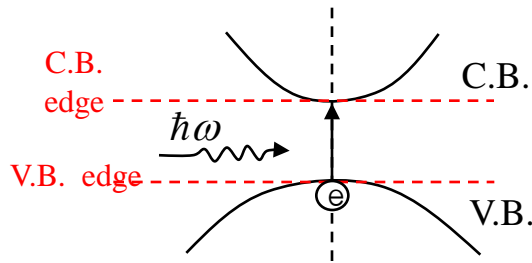
Direct Bandgap

- Measurement of band gap: Optical absorption



The threshold of continuous optical absorption at frequency ω_g determines the bandgap $E_g = \hbar\omega_g$

- Crystal with Direct Gap

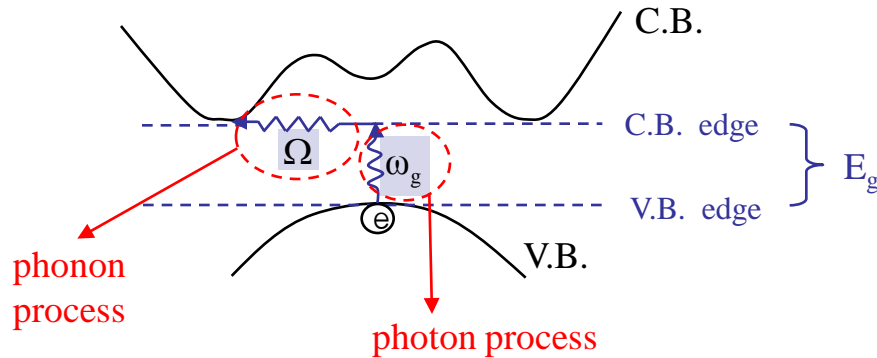


→ In the direct absorption process, a photon is absorbed by the crystal with the creation of an electron and a hole.

http://hynsr.korea.ac.kr/lecture/solid_state_physics/

Indirect Bandgap

- Crystal with Indirect Gap



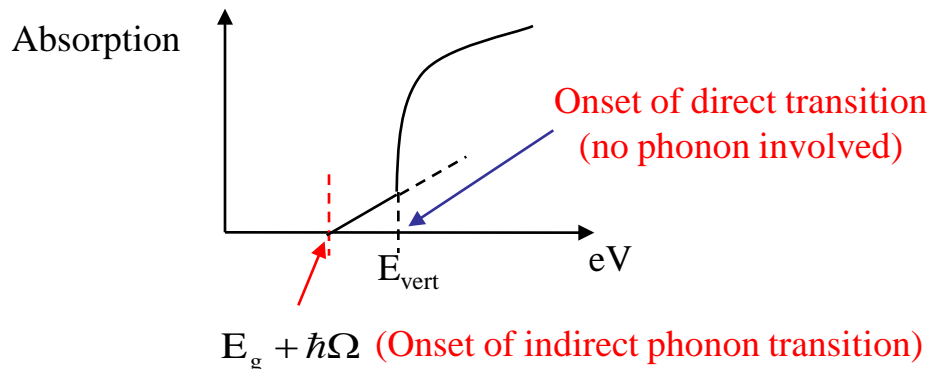
$$\therefore \hbar\omega (\text{photon}) = E_g + \hbar\Omega$$

Phonon energy involved.

In general

$$E_g \gg \hbar\Omega \quad (\sim 0.01 \text{ eV} - 0.03 \text{ eV})$$

- Optical absorption



http://hynsr.korea.ac.kr/lecture/solid_state_physics/

Direct Bandgap and Indirect Bandgap

Kittel, Solid State Physics (Chapter 8).

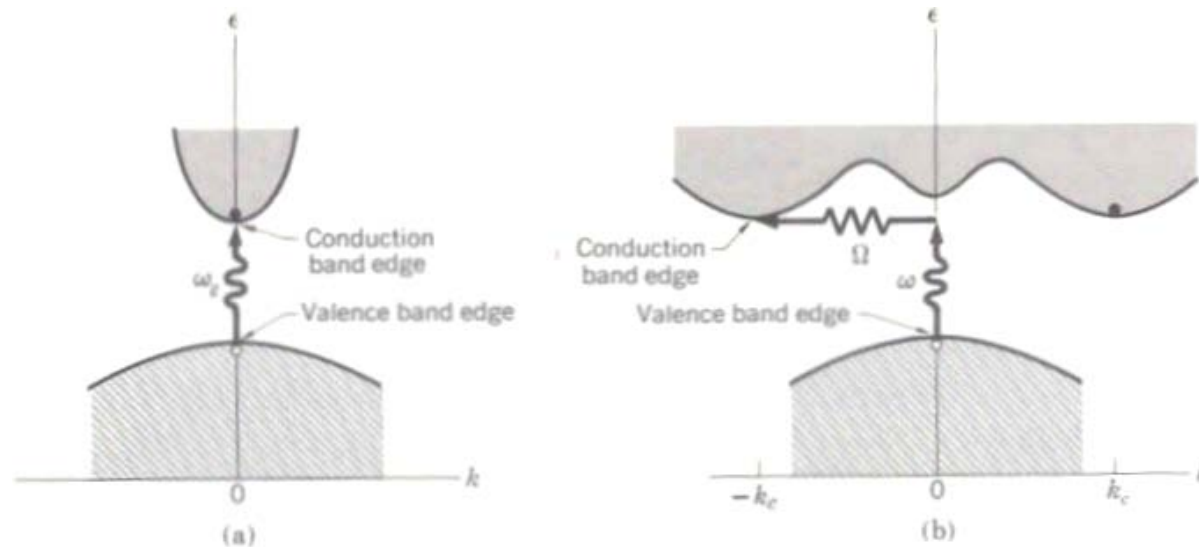
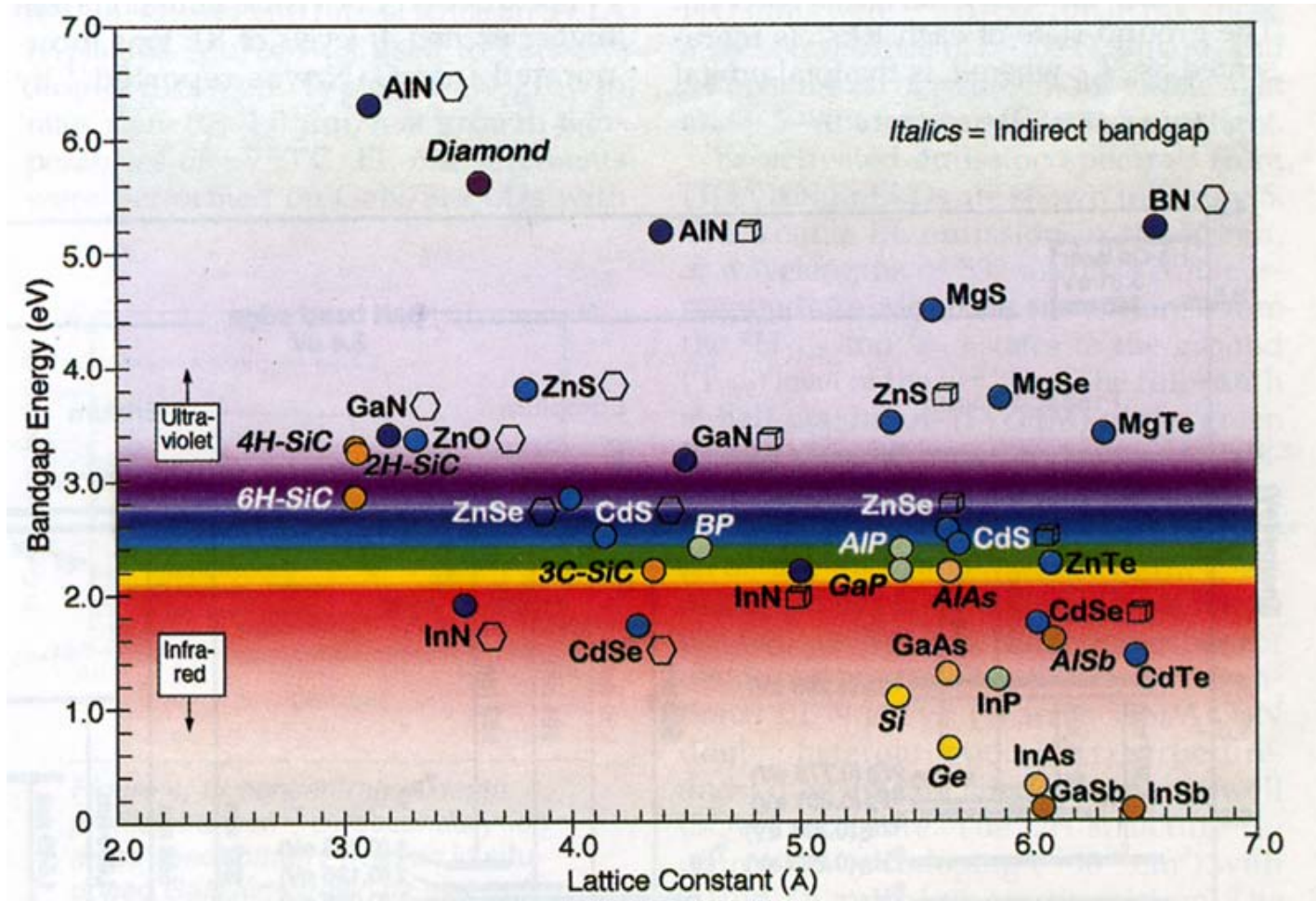


Figure 5 In (a) the lowest point of the conduction band occurs at the same value of k as the highest point of the valence band. A direct optical transition is drawn vertically with no significant change of k , because the absorbed photon has a very small wavevector. The threshold frequency ω_s for absorption by the direct transition determines the energy gap $E_g = \hbar\omega_s$. The indirect transition in (b) involves both a photon and a phonon because the band edges of the conduction and valence bands are widely separated in k space. The threshold energy for the indirect process in (b) is greater than the true band gap. The absorption threshold for the indirect transition between the band edges is at $\hbar\omega = E_g + \hbar\Omega$, where Ω is the frequency of an emitted *phonon* of wavevector $\mathbf{K} = -\mathbf{k}_c$. At higher temperatures phonons are already present; if a phonon is absorbed along with a photon, the threshold energy is $\hbar\omega = E_g - \hbar\Omega$. *Note:* The figure shows only the threshold transitions. Transitions occur generally between almost all points of the two bands for which the wavevectors and energy can be conserved.

Bandgap Energy for Semiconductors



MRS Bulletin (1999)

n-Type and p-Type Doping

Kittel, Solid State Physics (Chapter 8).

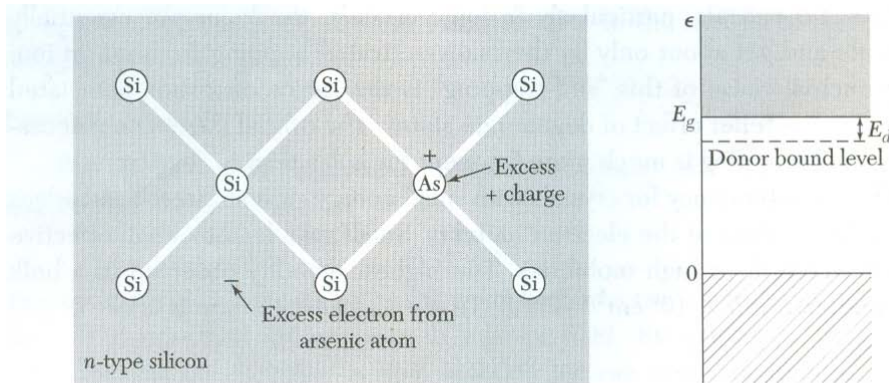


Figure 19 Charges associated with an arsenic impurity atom in silicon. Arsenic has five valence electrons, but silicon has only four valence electrons. Thus four electrons on the arsenic form tetrahedral covalent bonds similar to silicon, and the fifth electron is available for conduction. The arsenic atom is called a **donor** because when ionized it donates an electron to the conduction band.

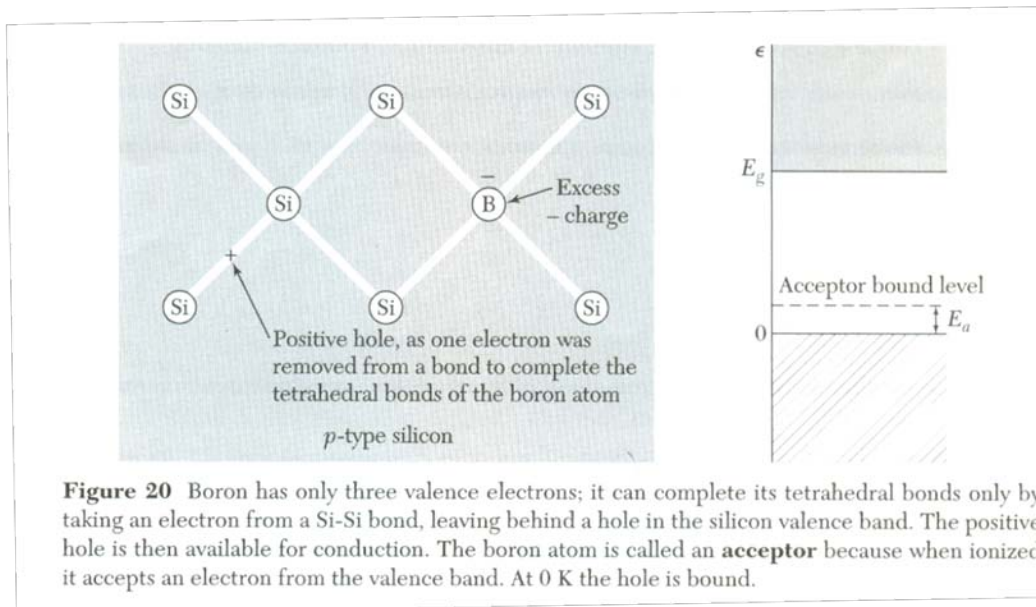
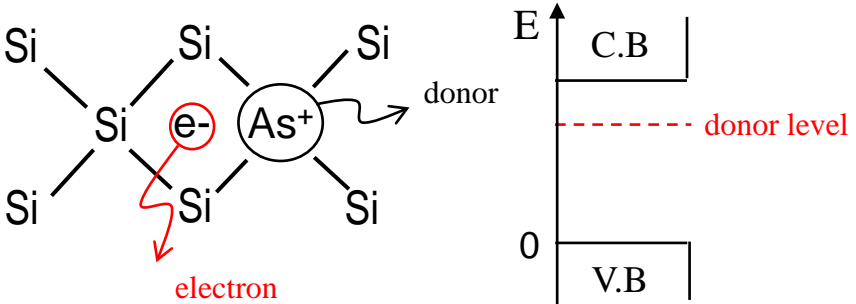
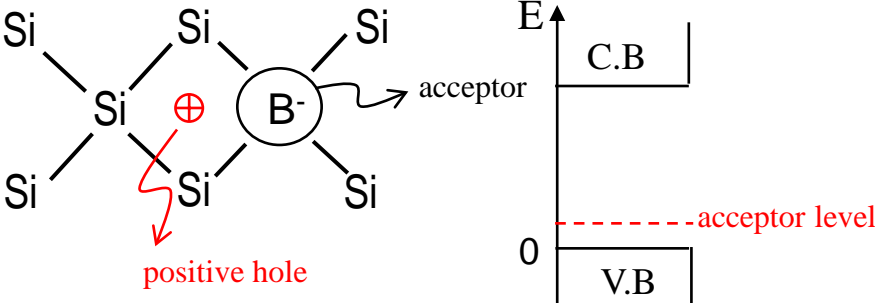


Figure 20 Boron has only three valence electrons; it can complete its tetrahedral bonds only by taking an electron from a Si-Si bond, leaving behind a hole in the silicon valence band. The positive hole is then available for conduction. The boron atom is called an **acceptor** because when ionized it accepts an electron from the valence band. At 0 K the hole is bound.

Donor state (<i>n</i> -type semiconductor)	Acceptor state (<i>p</i> -type semiconductor)
<p>→By donor, an excess electron exists near to the conduction band.</p>  <p>Donors (Electrons increased)</p> <p>P As Sb } Column V elements</p>	<p>→By acceptor, a positive hole exists near to the valence band.</p>  <p>Acceptors (Holes increased)</p> <p>B Ga In Al } Column III elements</p>

- Carrier Concentration

$$n = \int D(\varepsilon) f(\varepsilon) d\varepsilon$$

DOS

Fermi-Dirac distribution

$$n = 2 \left(\frac{m_e k_B T}{2\pi\hbar^2} \right)^{\frac{3}{2}} \exp[(E_F - E_C) / k_B T]$$

$$np = 4 \left(\frac{k_B T}{2\pi\hbar^2} \right)^3 (m_e m_h)^{\frac{3}{2}} \exp(-E_g / k_B T)$$

$$p = \int_{-\infty}^{E_v} D_h(\varepsilon) f_h(\varepsilon) d\varepsilon \quad f_h = 1 - f_e$$

$$p = 2 \left(\frac{m_h k_B T}{2\pi\hbar^2} \right)^{\frac{3}{2}} \exp[(E_v - E_F) / k_B T]$$

→ ‘n-p’ constant and independent of impurity concentration at a given temperature.

$$n_i = p_i = 2 \left(\frac{k_B T}{2\pi\hbar^2} \right)^{\frac{3}{2}} (m_e m_h)^{\frac{3}{4}} \exp(-E_g / 2k_B T)$$

$$E_F = \frac{1}{2} E_g + \frac{3}{4} k_B T \ln \left(\frac{m_h}{m_e} \right)$$



$$\left\{ \begin{array}{l} \textcircled{1} m_e = m_h \longrightarrow E_F = \frac{1}{2} E_g \\ \textcircled{2} T = 0 \end{array} \right.$$

The Fermi level is on the middle of E_g

- Intrinsic conductivity & carrier concentration (n) controlled by $\rightarrow \frac{E_g}{k_B T}$
 $\frac{E_g}{k_B T}$ is large \rightarrow the concentration of intrinsic carrier \rightarrow low
the conductivity \rightarrow low

Fermi-Dirac distribution

$$\frac{1}{\exp[(\epsilon - \mu)/k_B T] + 1}$$

If $\epsilon - \mu \gg k_B T$,

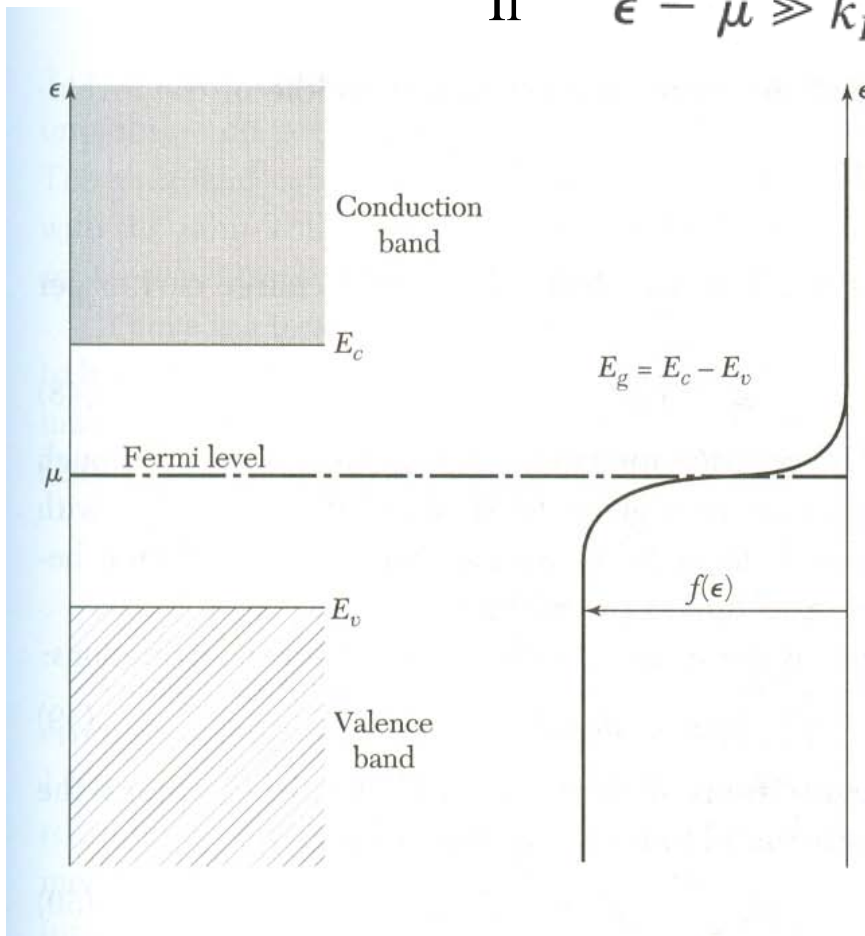
$$f_e \approx \exp[(\mu - \epsilon)/k_B T]$$

$$\epsilon_k = E_c + \frac{\hbar^2 k^2}{2m_e}$$

$$D_e(\epsilon) = \frac{1}{2\pi^2} \left(\frac{2m_e}{\hbar^2} \right)^{3/2} (\epsilon - E_c)^{1/2}$$

Density of State for Electron

Figure 18. Energy scale for statistical calculations. The Fermi distribution function is shown on the same scale, for a temperature $k_B T \ll E_g$. The Fermi level μ is taken to lie well within the band gap, as for an intrinsic semiconductor. If $\epsilon = \mu$, then $f = \frac{1}{2}$.



Intrinsic Carrier Concentration

$$n = \int_{E_c}^{\infty} D_e(\epsilon) f_e(\epsilon) d\epsilon = \frac{1}{2\pi^2} \left(\frac{2m_e}{\hbar^2} \right)^{3/2} \exp(\mu/k_B T) \times \int_{E_c}^{\infty} (\epsilon - E_c)^{1/2} \exp(-\epsilon/k_B T) d\epsilon ,$$

Thus
$$n = 2 \left(\frac{m_e k_B T}{2\pi \hbar^2} \right)^{3/2} \exp[(\mu - E_c)/k_B T]$$

$$f_h = 1 - f_e, \quad \text{If } (\mu - \epsilon) \gg k_B T$$

$$f_h = 1 - \frac{1}{\exp[(\epsilon - \mu)/k_B T] + 1} = \frac{1}{\exp[(\mu - \epsilon)/k_B T] + 1} \cong \exp[(\epsilon - \mu)/k_B T] ,$$

$$D_h(\epsilon) = \frac{1}{2\pi^2} \left(\frac{2m_h}{\hbar^2} \right)^{3/2} (E_v - \epsilon)^{1/2}$$

Kittel, Solid State Physics (Chapter 8).

Intrinsic Carrier Concentration

Thus
$$p = \int_{-\infty}^{E_c} D_h(\epsilon) f_h(\epsilon) d\epsilon = 2 \left(\frac{m_h k_B T}{2\pi\hbar^2} \right)^{3/2} \exp[(E_c - \mu)/k_B T]$$

$$np = 4 \left(\frac{k_B T}{2\pi\hbar^2} \right)^3 (m_c m_h)^{3/2} \exp(-E_g/k_B T)$$

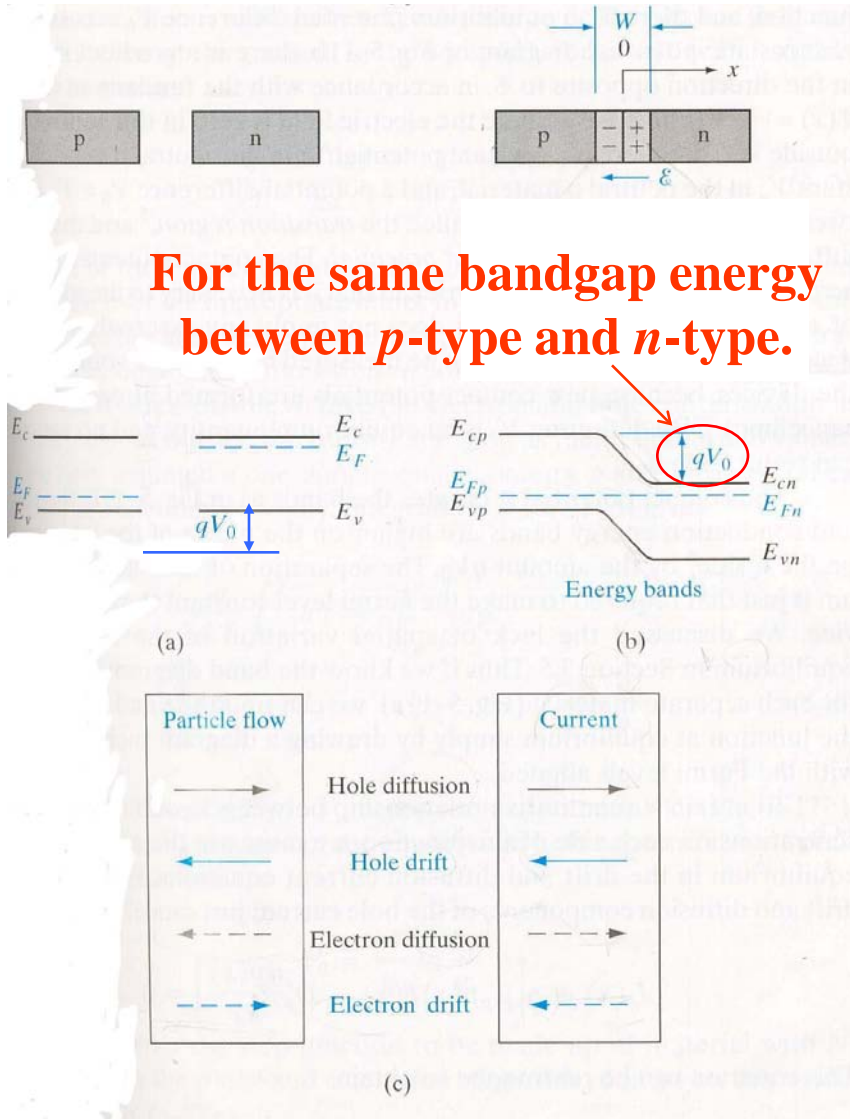
$$n_i = p_i = 2 \left(\frac{k_B T}{2\pi\hbar^2} \right)^{3/2} (m_e m_h)^{3/4} \exp(-E_g/2k_B T)$$

$$\exp(2\mu/k_B T) = (m_h/m_e)^{3/2} \exp(E_g/k_B T)$$

$$\mu = \frac{1}{2} E_g + \frac{3}{4} k_B T \ln(m_h/m_e) .$$

Kittel, Solid State Physics (Chapter 8).

Properties of an Equilibrium p - n Junction



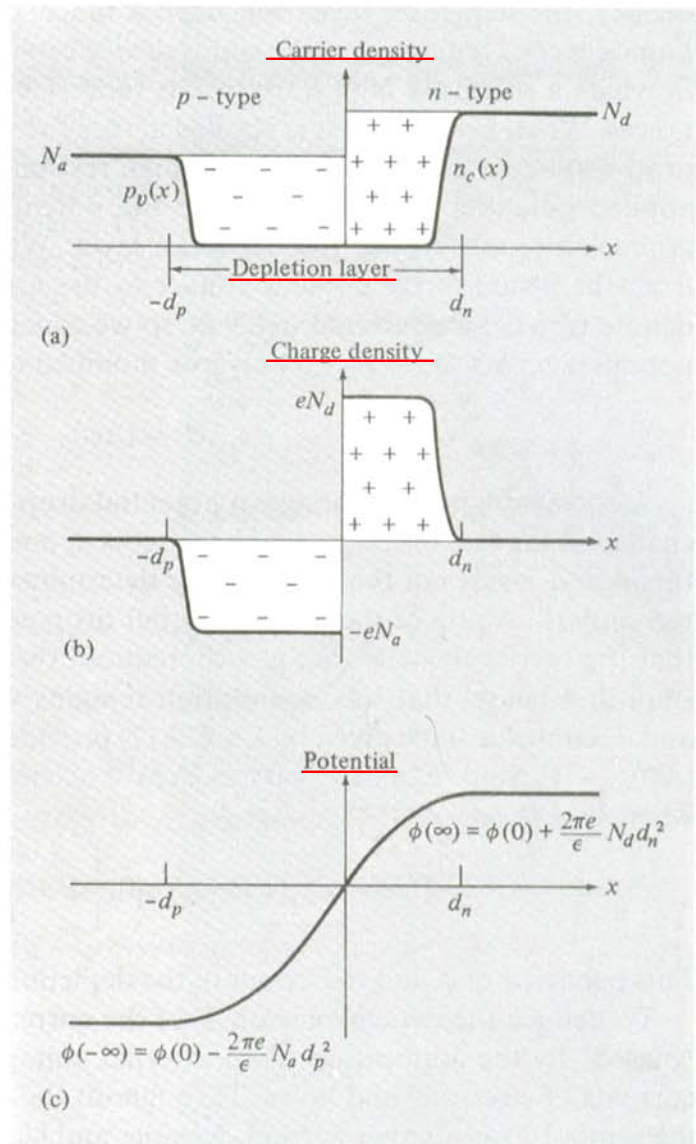
- (a) Isolated, neutral regions of p -type and n -type material and energy bands for the isolated regions
- (b) Junction, showing space charge in the transition region W , the resulting electric field \mathcal{E} and contact potential V_0 , and the separation of the energy band.
- (c) Directions of the four components of particle flow within the transition region, and the resulting current directions.

Solid State Electronic Devices (6th edition, Chapter 5)
B. G. Streetman and S. K. Banerjee

Depletion Layer

Figure 29.3

(a) Carrier densities, (b) charge density, and (c) potential $\phi(x)$ plotted vs. position across an abrupt p - n junction. In the analysis in the text the approximation was made that the carrier densities and charge density are constants except for discontinuous changes at $x = -d_p$ and $x = d_n$. More precisely (see Problem 1), these quantities undergo rapid change over regions just within the depletion layer whose extent is a fraction of order $(k_B T/E_g)^{1/2}$ of the total extent of the depletion layer. The extent of the depletion layer is typically from 10^2 to 10^4 Å.



$$\sigma(x)$$

$$\rho(x)$$

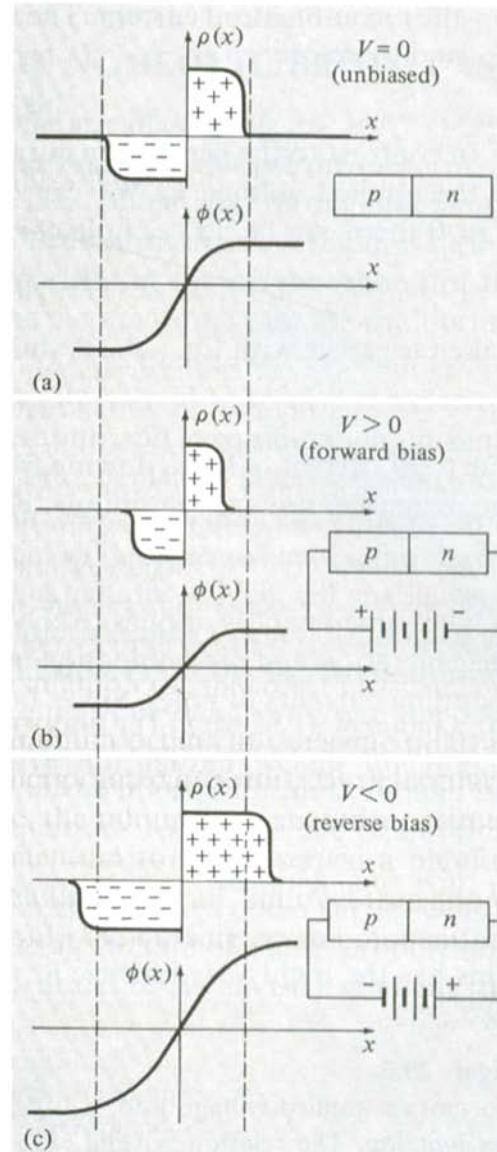
$$\Phi(x)$$

Ashcroft, Solid State Physics

Carrier Density at a p-n Junction

Figure 29.4

The charge density ρ and potential ϕ in the depletion layer (a) for the unbiased junction, (b) for the junction with $V > 0$ (forward bias), and (c) for the junction with $V < 0$ (reverse bias). The positions $x = d_n$ and $x = -d_p$ that mark the boundaries of the depletion layer when $V = 0$ are given by the dashed lines. The depletion layer and change in ϕ are reduced by a forward bias and increased by a reverse bias.



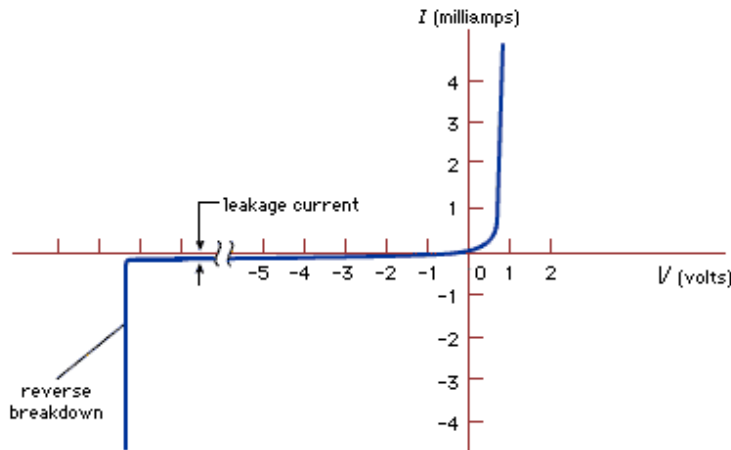
Equilibrium

Forward bias

Reverse bias

Ashcroft, Solid State Physics

A Typical Silicon p-n Junction



Typical한 Si diode에서는 ideal 한 I - V characteristic 이 보인다.

applied forward voltage 는 보통 1 V 보다 작고, breakdown voltage는 impurity concentration 과 다른 parameter에 따라 1 V 보다 작은 값에서부터 수천 voltage 까지 변할 수 있다.

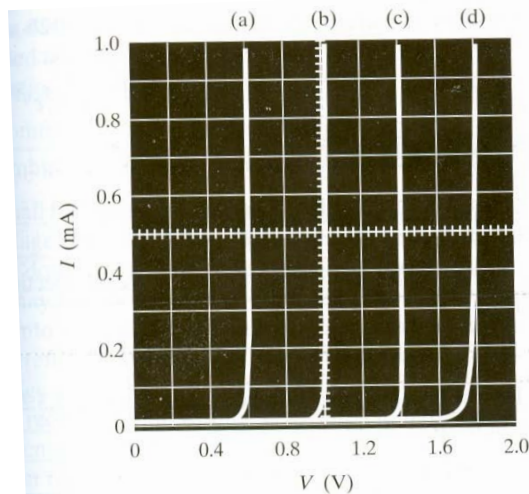


Figure 5-33
 I - V characteristics of heavily doped p-n junction diodes at 77 K, illustrating the effects of contact potential on the forward current: (a) Ge, $E_g \approx 0.7$ eV; (b) Si, $E_g \approx 1.1$ eV; (c) GaAs, $E_g \approx 1.4$ eV; (d) GaAsP, $E_g \approx 1.9$ eV.

77 K에서 Ge, Si, GaAs, GaAsP diode의 I - V curve.

heavy doping되어 p-type 쪽과 n-type 쪽의 Fermi level이 각각 valence band와 conduction 에 거의 근접했다고 가정하였을 때, 각 물질의 band gap energy에 가까운 voltage가 가해지면 current가 급격히 증가한다.

Solid State Electronic Devices (6th edition, Chapter 5)
 Ben G. Streetman, Sanjay Kumar Banerjee

Type-I and Type-II Band-Edge Alignment

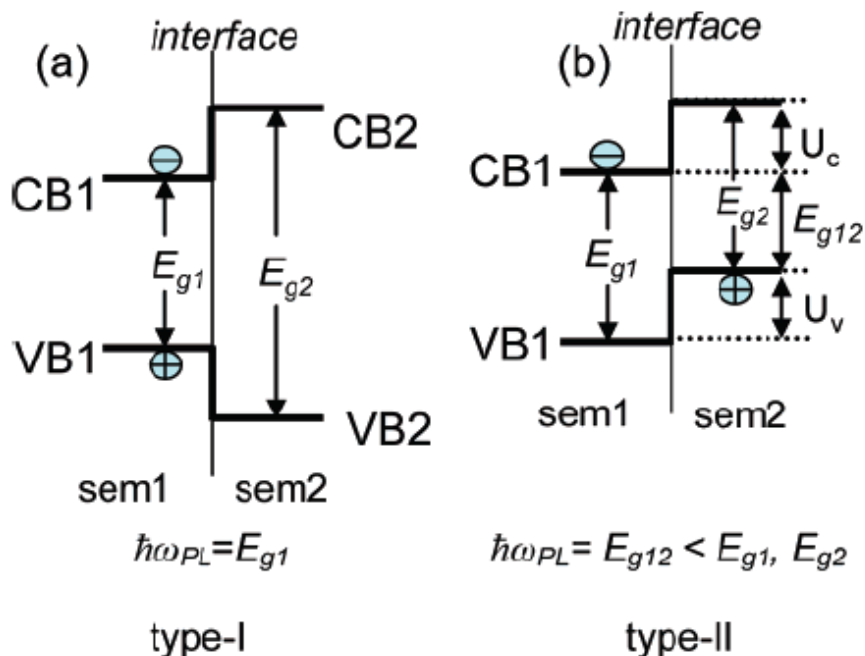


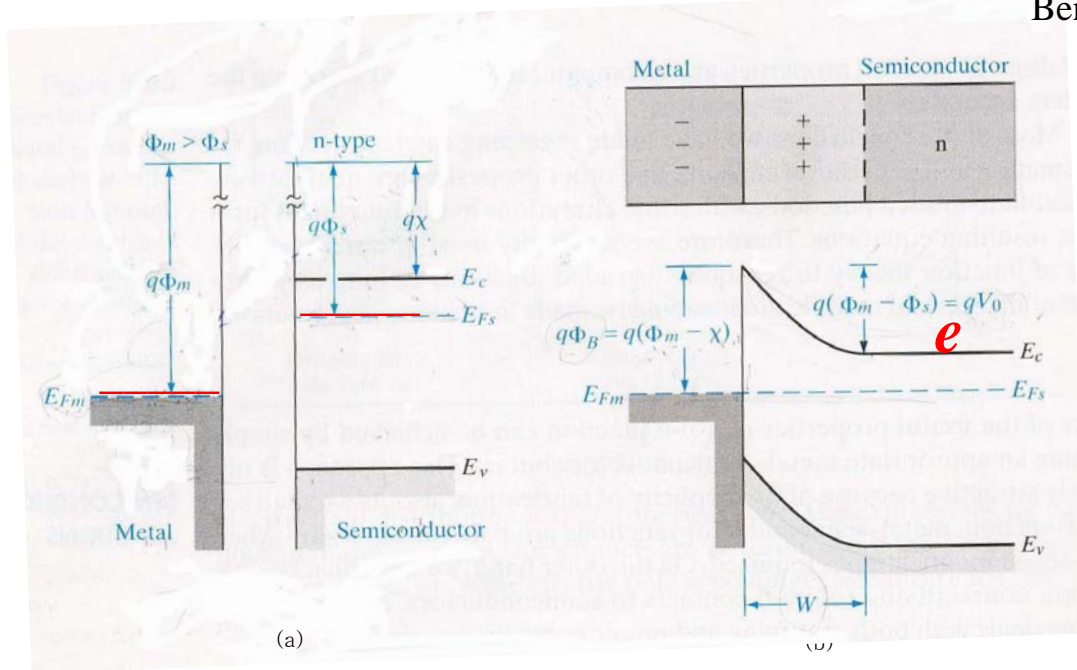
Figure 1. Type-I (a) and type-II (b) band-edge alignments at the heterointerface between two semiconductors. In the type-I structure, both an electron and a hole tend to localize within the material with a narrower energy gap, which is semiconductor 1 (*sem1*) in the present case. As a result, the emission energy, $\hbar\omega_{PL}$, is determined by E_{g1} . The energy gradient existing in the type-II structure tends to spatially separate the electron and the hole on different sides of the heterointerface. In this case, the emission energy is determined by the energy difference between the conduction band edge of *sem1* and the valence band edge of semiconductor 2 (*sem2*), and hence, it is lower than the band gap of either semiconductor.

Semiconductor heterostructures are typically classified as type-I or type-II, depending on the relative alignment of conduction- and valence-band edges of the materials that are combined at the heterointerface. In the type-I structures, both the conduction and the valence band edges of one semiconductor (semiconductor 1 in Figure 1a) are located within the energy gap of the other semiconductor (semiconductor 2 in Figure 1a). In this case, an electron–hole (e–h) pair excited near the interface tends to localize in semiconductor 1, which provides the lowest energy states for both electrons and holes. In the type-II case (Figure 1b), the lowest energy states for electrons and holes are in different semiconductors; therefore, the energy gradient existing at the interfaces tends to spatially separate electrons and holes on different sides of the heterojunction. The corresponding “spatially indirect” energy gap (E_{g12}) is determined by the energy separation between the conduction-band edge of one semiconductor and the valence-band edge of the other semiconductor. For the case shown in Figure 1b, E_{g12} can be related to conduction (U_c) and valence (U_v) band energy offsets at the interface by $E_{g12} = E_{g1} - U_v = E_{g2} - U_c$, where E_{g1} and E_{g2} are the band gaps of semiconductors 1 and 2, respectively.

V. I. Klimov, Los Alamos National Laboratory
J. Am. Chem. Soc. (2007)

Schottky Barriers

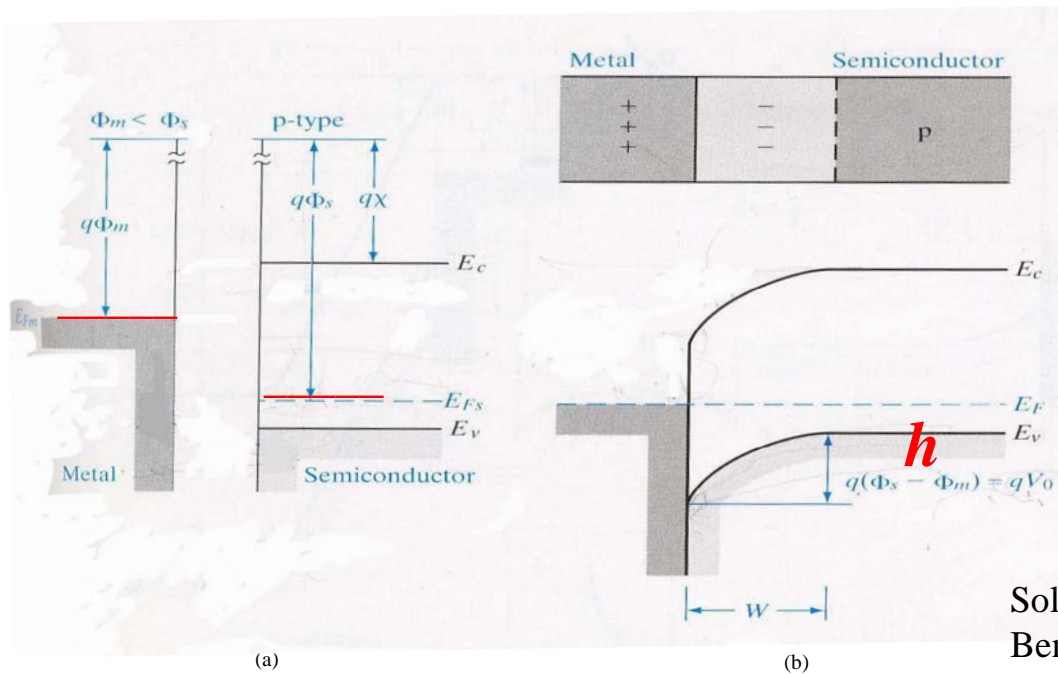
Solid State Electronic Devices (6th edition, Chapter 5)
Ben G. Streetman, Sanjay Kumar Banerjee



A Schottky barrier formed by contacting on *n*-type semiconductor with a metal having a larger work function:

- (a) Band diagrams for the metal and the semiconductor before joining.
- (b) Equilibrium band diagram for the junction.

Schottky Barriers



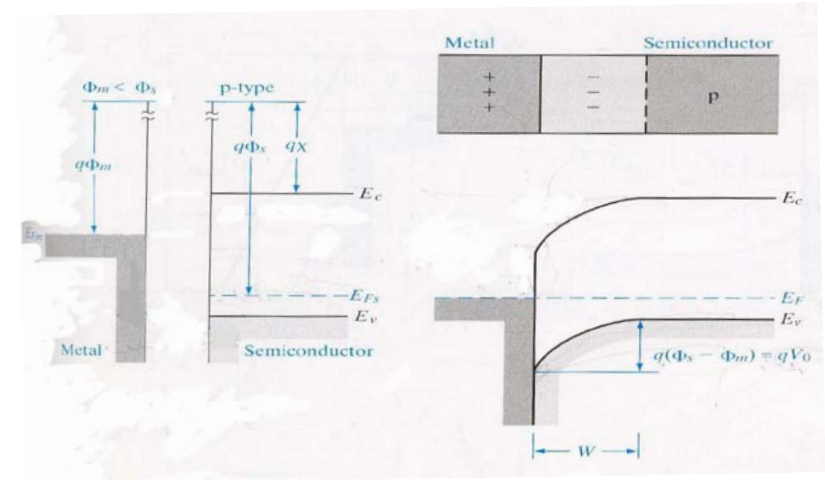
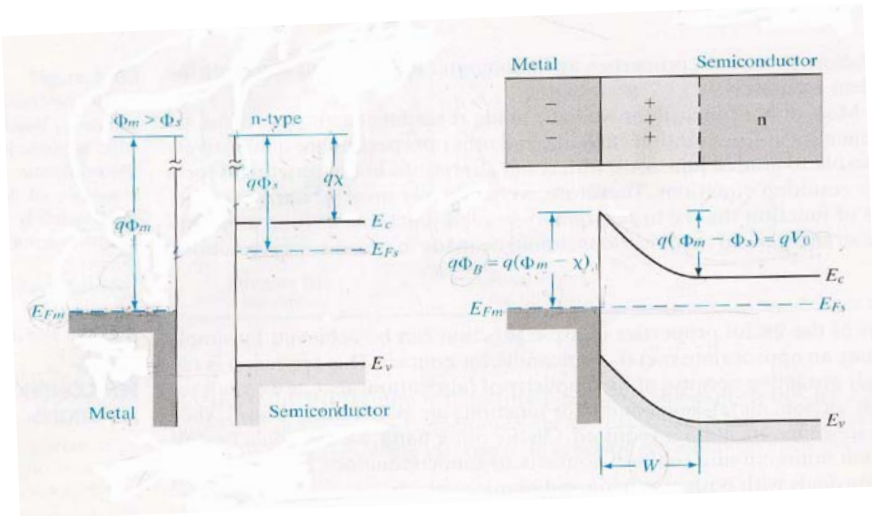
Solid State Electronic Devices (6th edition, Chapter 5)
Ben G. Streetman, Sanjay Kumar Banerjee

A Schottky barrier between a *p*-type semiconductor and a metal having a smaller work function:

(a) Band diagrams before joining.

(b) Band diagram for the junction at equilibrium.

A Feature of Schottky Barriers



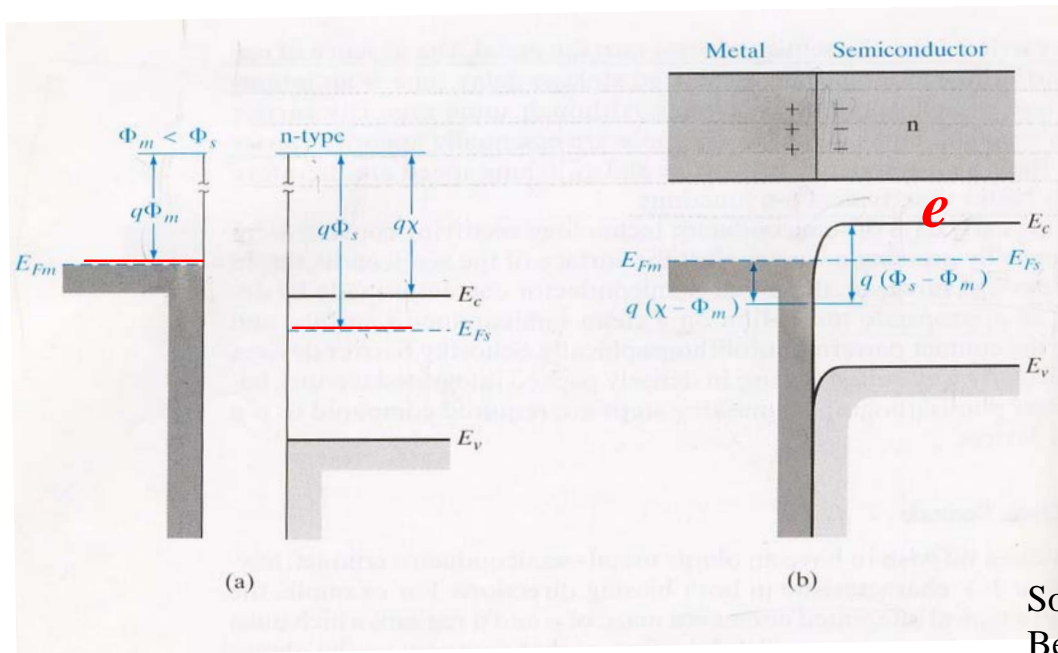
Solid State Electronic Devices (6th edition, Chapter 5)
Ben G. Streetman, Sanjay Kumar Banerjee

The absence of minority carrier injection.

Since the forward current in each case is due to the injection of majority carriers from the semiconductor into the metal.

→ Switching speed of Schottky barriers is generally better than *p-n* junction.

Ohmic Contact



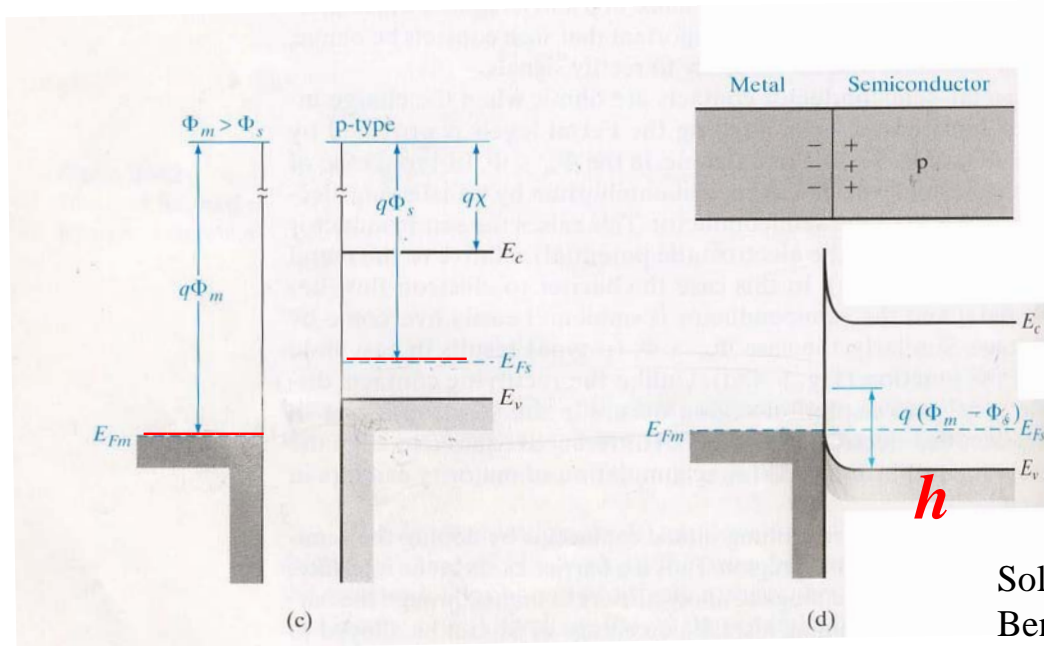
Solid State Electronic Devices (6th edition, Chapter 5)
Ben G. Streetman, Sanjay Kumar Banerjee

Ohmic metal-semiconductor contacts:

(a) $q\Phi_m < q\Phi_s$ for an *n*-type semiconductor.

(b) The equilibrium band diagram for the junction.

Ohmic Contact



Solid State Electronic Devices (6th edition, Chapter 5)
Ben G. Streetman, Sanjay Kumar Banerjee

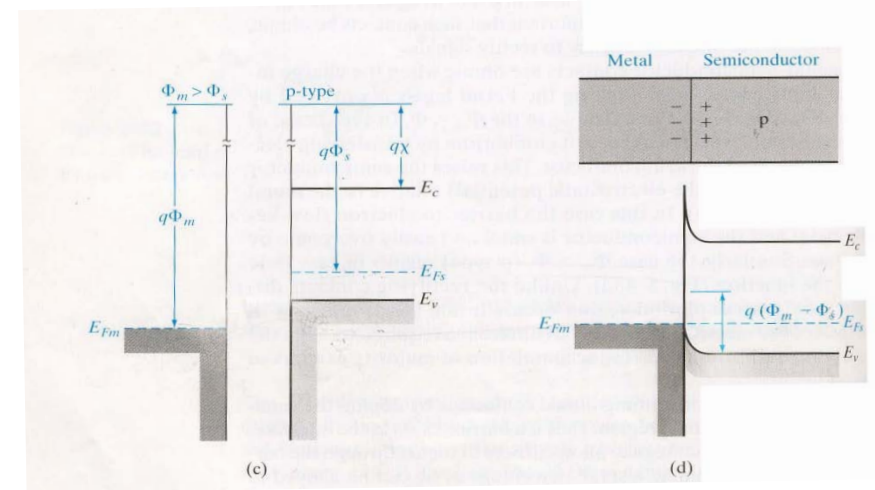
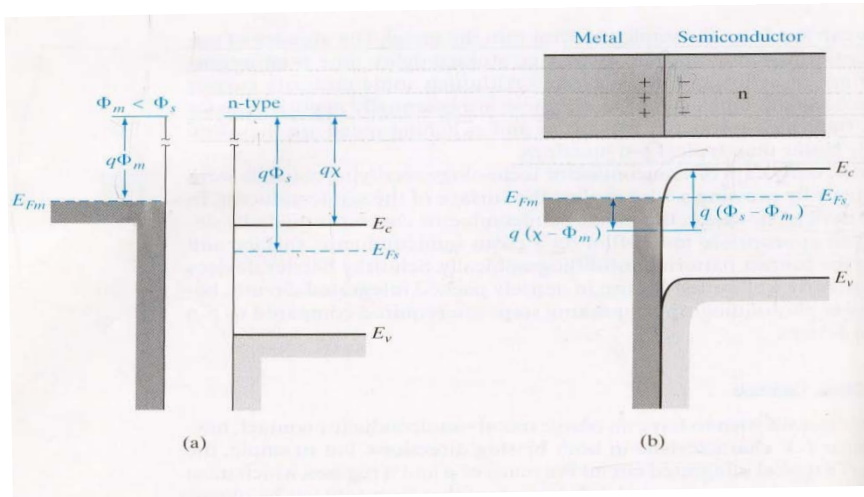
Ohmic metal-semiconductor contacts:

(a) $\Phi_m > \Phi_s$ for an p -type semiconductor.

(b) The equilibrium band diagram for the junction.

A Feature of Ohmic Contacts

Solid State Electronic Devices (6th edition, Chapter 5)
Ben G. Streetman, Sanjay Kumar Banerjee

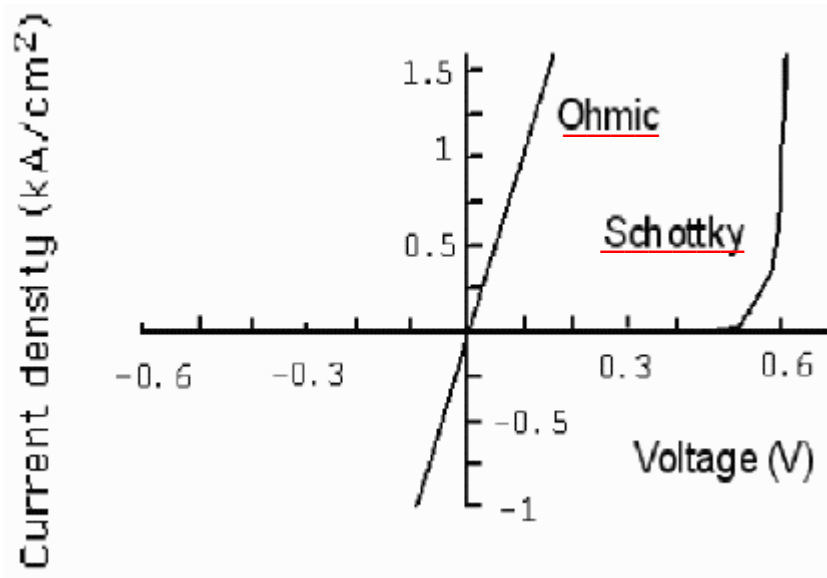


Linear I - V characteristics.

No depletion region.

Aligning the Fermi levels at equilibrium calls for accumulation of majority carriers in the semiconductor.

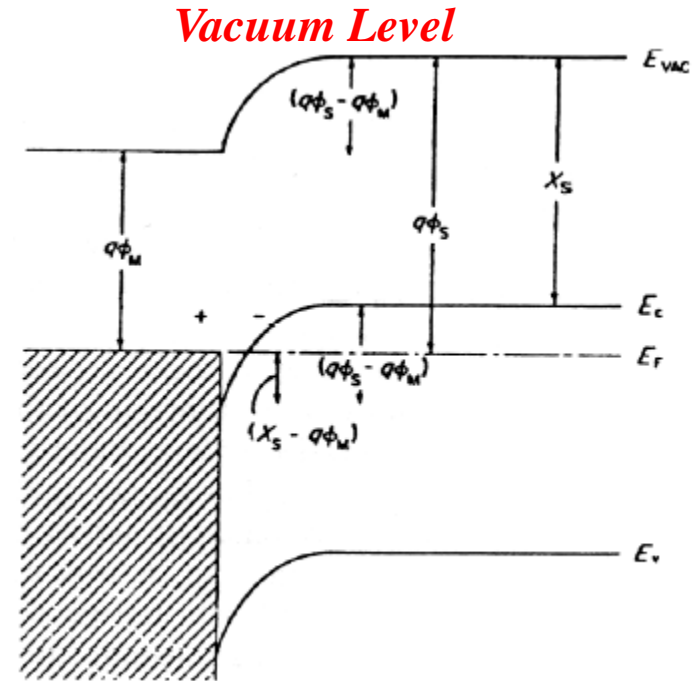
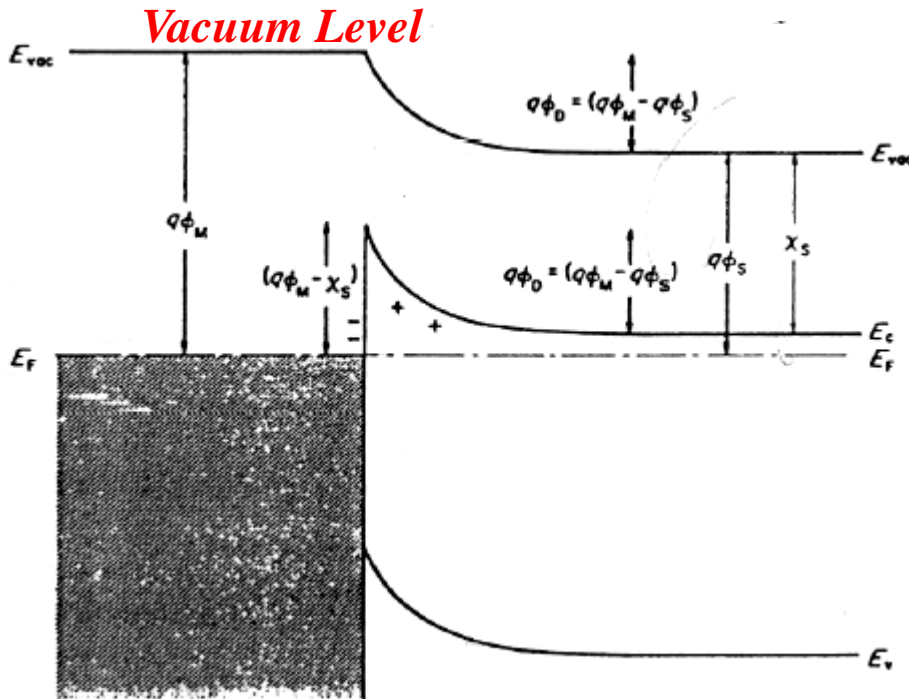
I-V Characteristics of Ohmic and Schottky Barriers



Current-voltage characteristics of Ohmic and Schottky barrier metal-semiconductor contacts to GaAs.

Schottky contact to GaAs is doped at 10^{15} cm^{-3} , and the Ohmic contact resistance is $10^4 \text{ } \Omega\text{cm}^2$.

http://www.mtmi.vu.lt/legacy/pfk/funkc_dariniai/diod/schottky.htm



Schottky junction (*n*-type semiconductor)

Ohmic junction (*n*-type semiconductor)

Barrier

Metal to semiconductor = $\Phi_M - \chi_S$

Semiconductor to metal = $\Phi_M - \Phi_S$

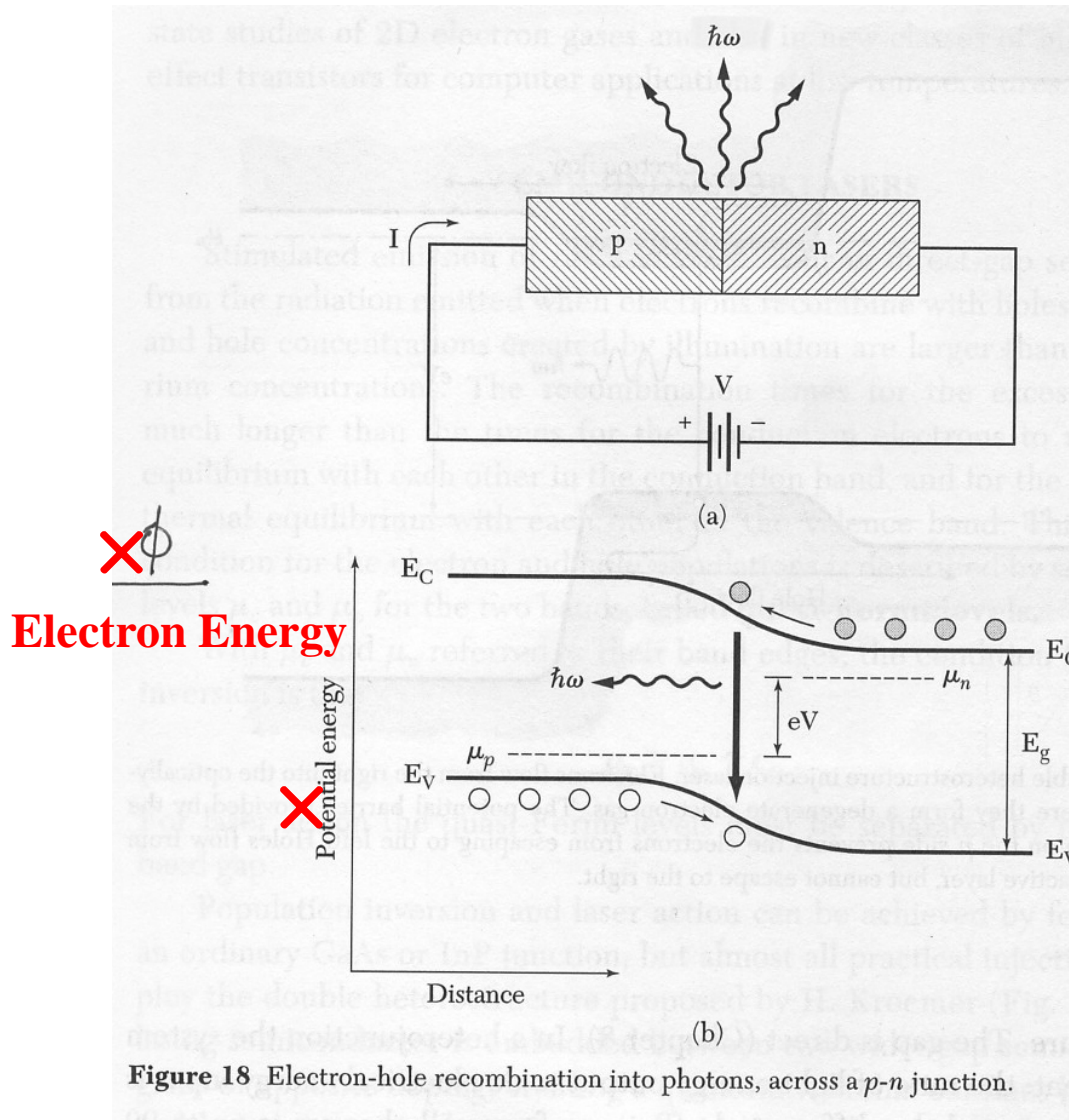
Negligible Barrier

depletion layer is

thin (1-3 atomic layer) at metal

Electron-Hole Recombination of a p-n Junction

Kittel, Solid State Physics (Chapter 17).



Double Heterostructure Injection Laser

Kittel, Solid State Physics (Chapter 17).

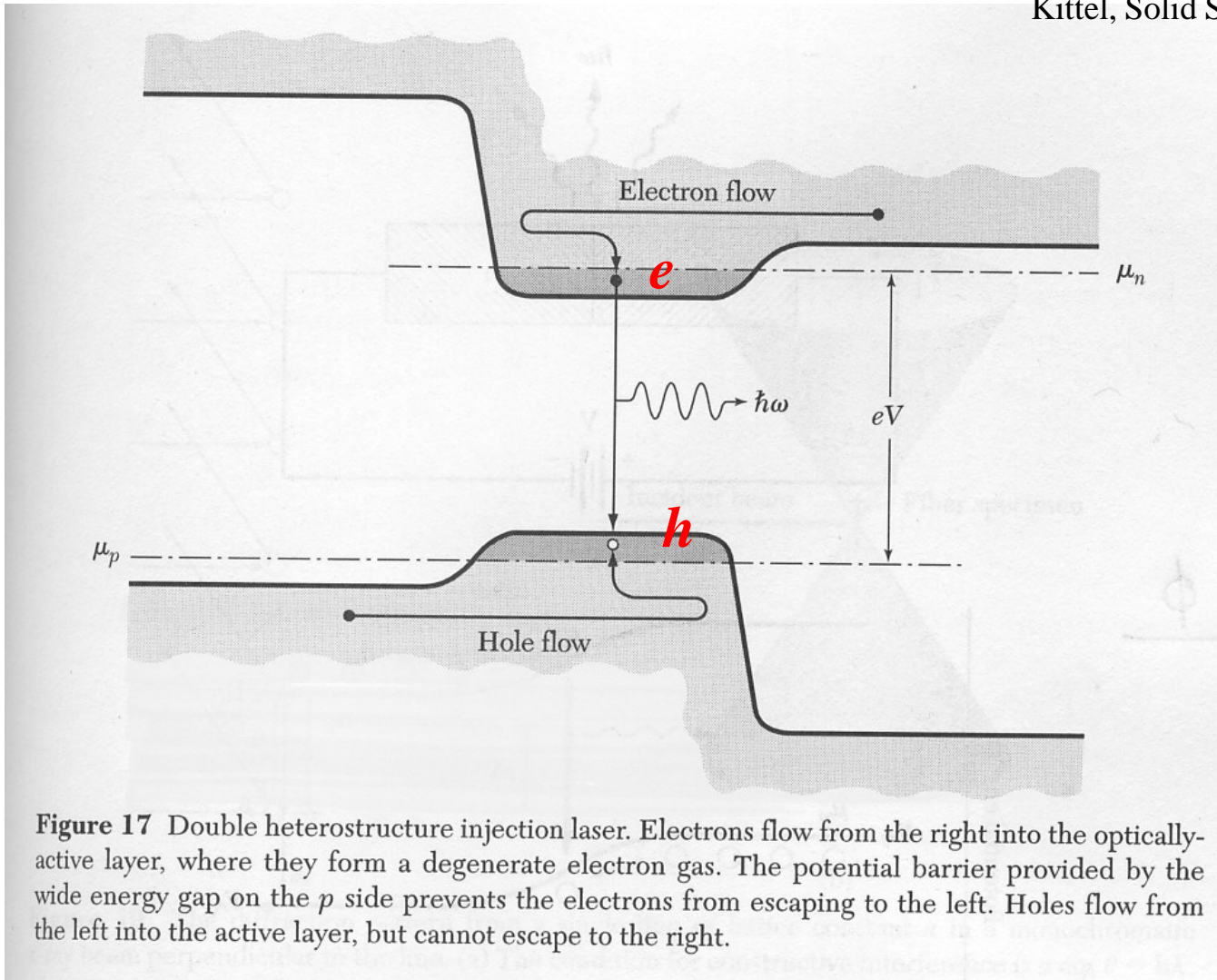


Figure 17 Double heterostructure injection laser. Electrons flow from the right into the optically-active layer, where they form a degenerate electron gas. The potential barrier provided by the wide energy gap on the p side prevents the electrons from escaping to the left. Holes flow from the left into the active layer, but cannot escape to the right.

Radiative and Nonradiative Recombination

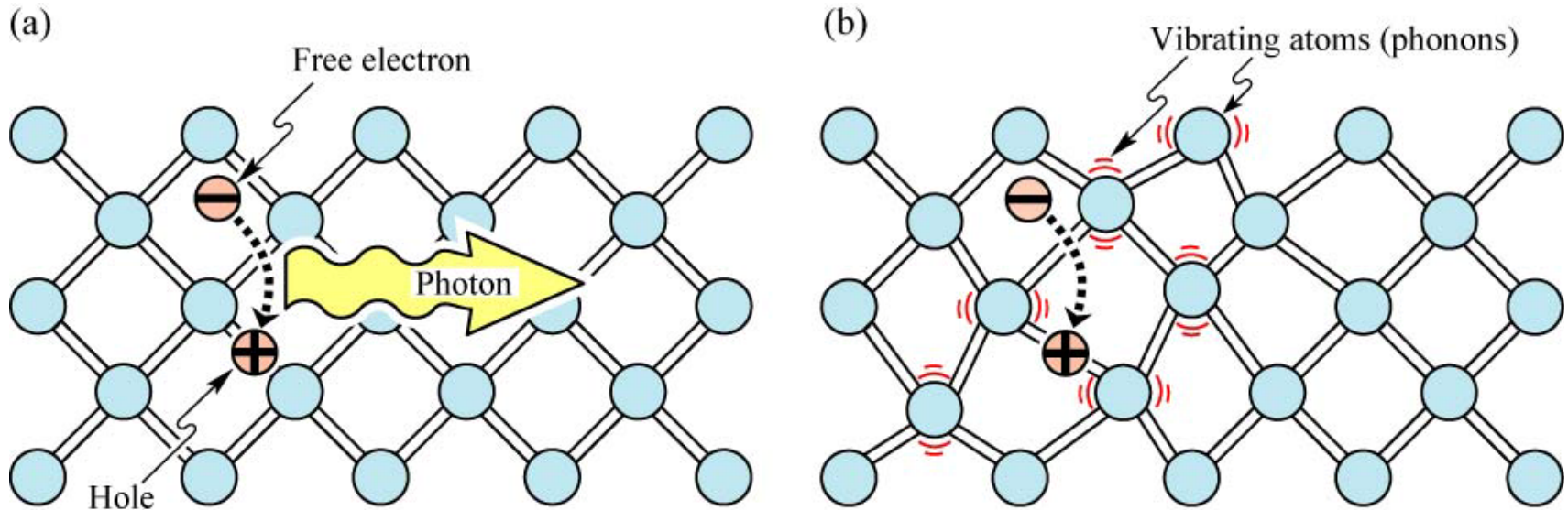


Fig. 2.5. (a) Radiative recombination of an electron-hole pair accompanied by the emission of a photon with energy $h\nu \approx E_g$. (b) In non-radiative recombination events, the energy released during the electron-hole recombination is converted to phonons (adopted from Shockley, 1950).

E. F. Schubert
Light-Emitting Diodes (Cambridge Univ. Press)
www.LightEmittingDiodes.org

$$\eta = \frac{k_{rad}}{k_{rad} + k_{nonrad}}$$

Effective Mass

$$\frac{dv_g}{dt} = \hbar^{-1} \frac{d^2\epsilon}{dk dt} = \hbar^{-1} \left(\frac{d^2\epsilon}{dk^2} \frac{dk}{dt} \right)$$

Thus
$$\frac{dv_g}{dt} = \left(\frac{1}{\hbar^2} \frac{d^2\epsilon}{dk^2} \right) F ;$$

We know that

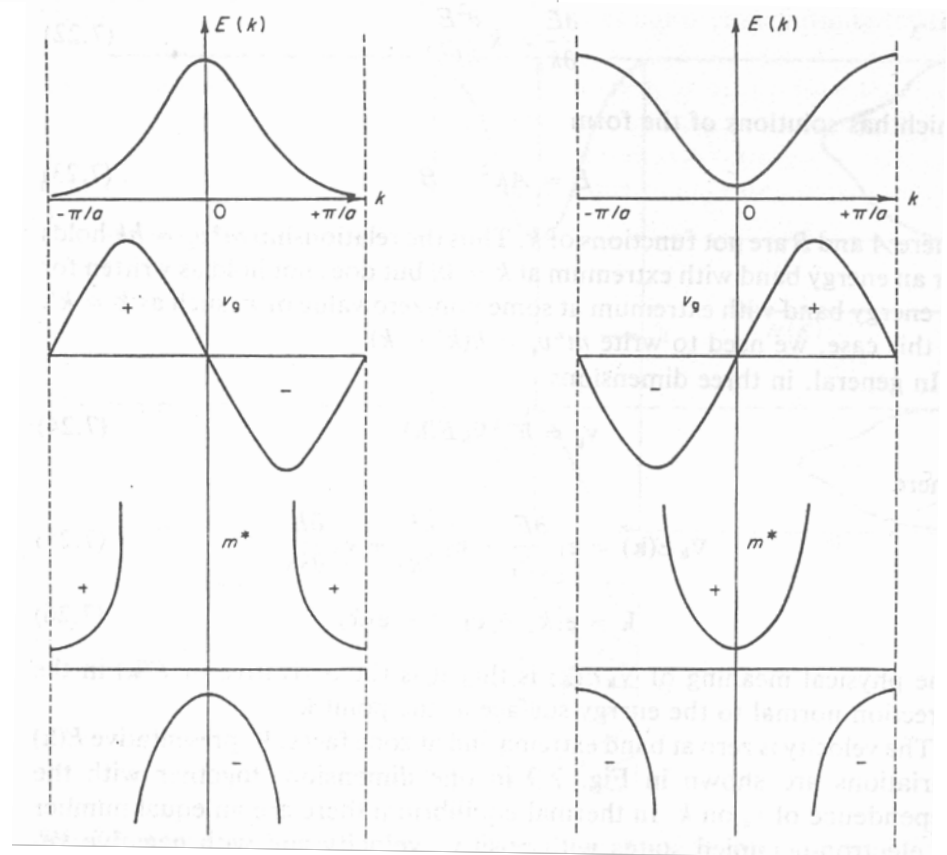
$$dk/dt = F/\hbar,$$

or
$$F = \frac{\hbar^2}{d^2\epsilon/dk^2} \frac{dv_g}{dt}$$

Effective mass m^*

$$\frac{1}{m^*} = \frac{1}{\hbar^2} \frac{d^2\epsilon}{dk^2} .$$

Typical variation of group velocity v_g and effective mass m^* as a function of k .



H. Bube, Electrons in Solids (Chapter 10)

Hole = Missing Electron

Kittel, Solid State Physics (Chapter 8)

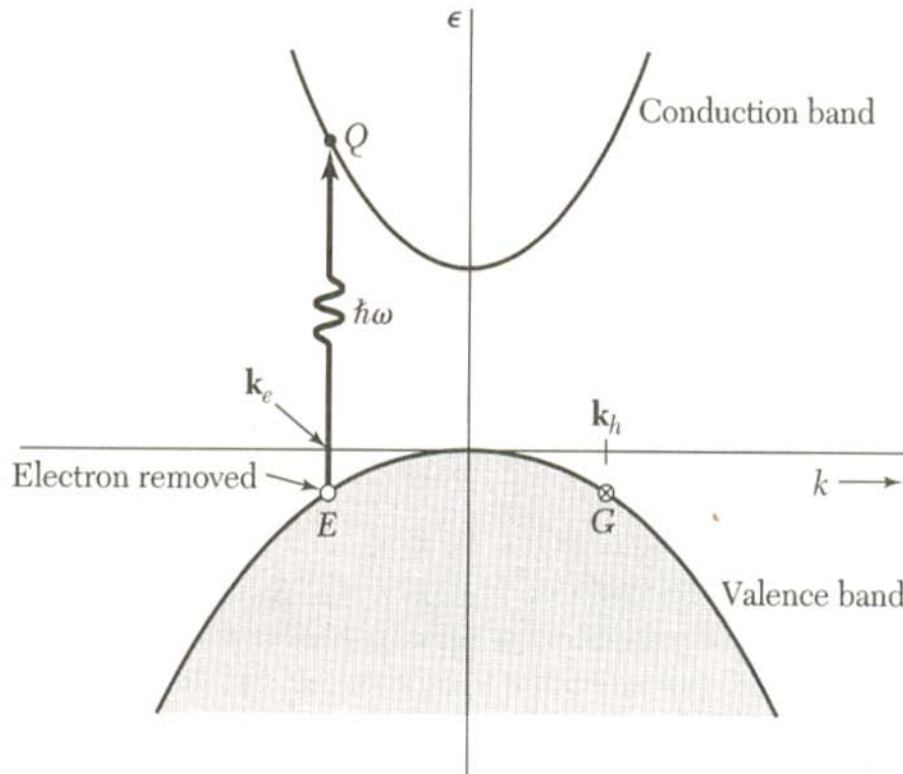
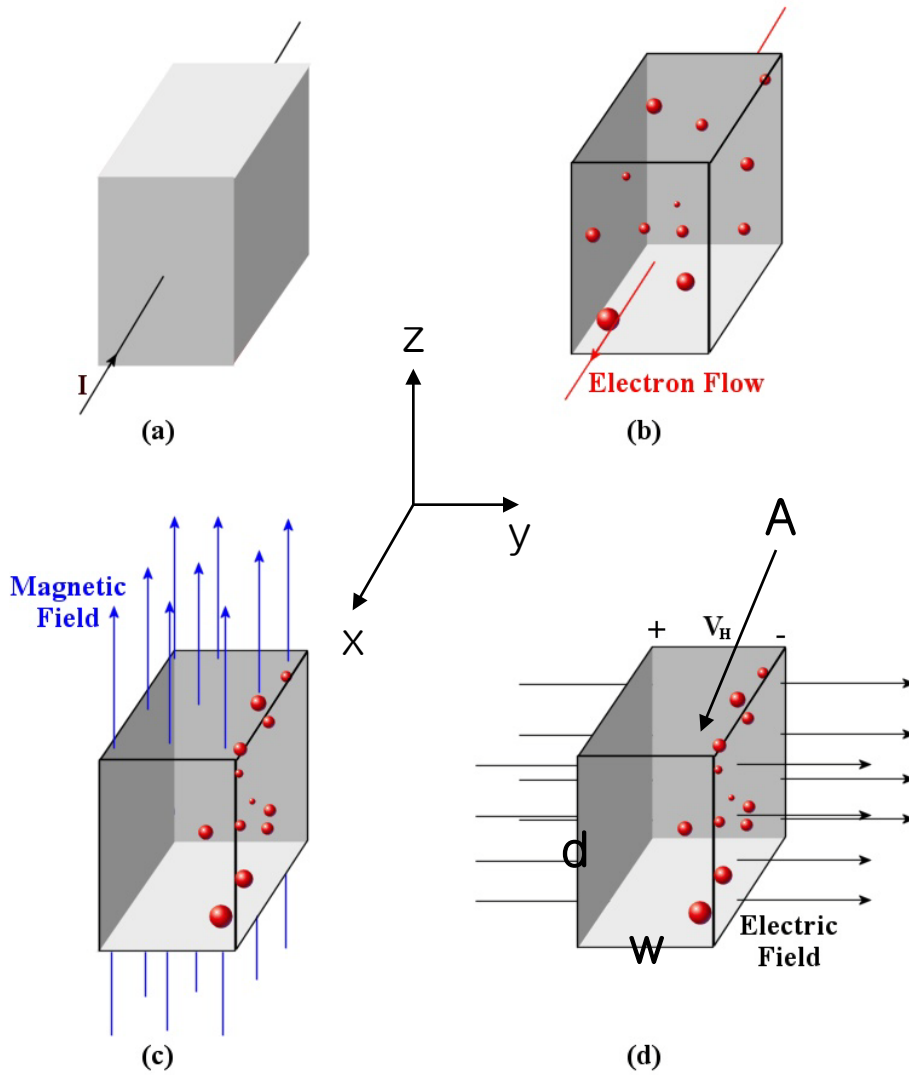


Figure 7 Absorption of a photon of energy $\hbar\omega$ and negligible wavevector takes an electron from E in the filled valence band to Q in the conduction band. If k_e was the wavevector of the electron at E , it becomes the wavevector of the electron at Q . The total wavevector of the valence band after the absorption is $-k_e$, and this is the wavevector we must ascribe to the hole if we describe the valence band as occupied by one hole. Thus $k_h = -k_e$; the wavevector of the hole is the same as the wavevector of the electron which remains at G . For the entire system the total wavevector after the absorption of the photon is $k_e + k_h = 0$, so that the total wavevector is unchanged by the absorption of the photon and the creation of a free electron and free hole.

Hall Measurement



Lorentz force induces charge accumulation at the $x - z$ plane:

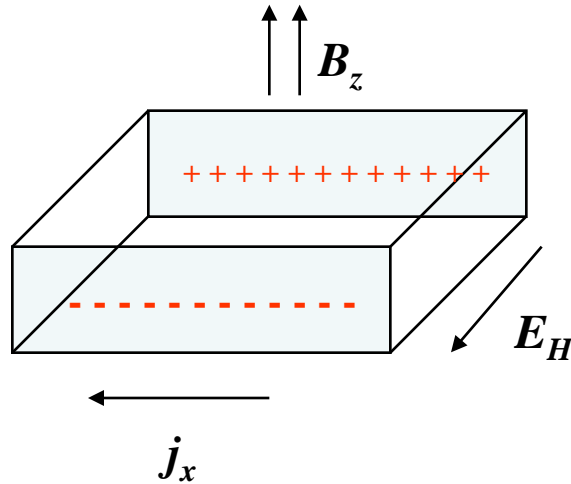
→ E_H field generation

Majority carrier and carrier density can be calculated by Hall measurement.

<http://en.wikipedia.org>

Hall Mobility

Kittel, Solid State Physics (Chapter 6, Eqs. 53 -55)



<Hall effect of *p*-type semiconductor>

$$\mu_H = \frac{p\mu_p^2 - n\mu_n^2}{p\mu_p + n\mu_n}$$

<by theoretical calculation>

$$\sigma = ne^2\tau/m = ne\mu_e$$

Electron mobility or hole mobility

Hall coefficient

$$R_H = \frac{E_H}{j_x B_z} = \frac{1}{nqc}$$

Hall mobility

$$\begin{aligned} \mu_H &= c\sigma R_H \\ &= cq(n\mu_e + p\mu_h) \frac{1}{nqc} \end{aligned}$$

(*n*-type)

$$\approx cq n \mu_e \frac{1}{nqc} = \mu_e$$

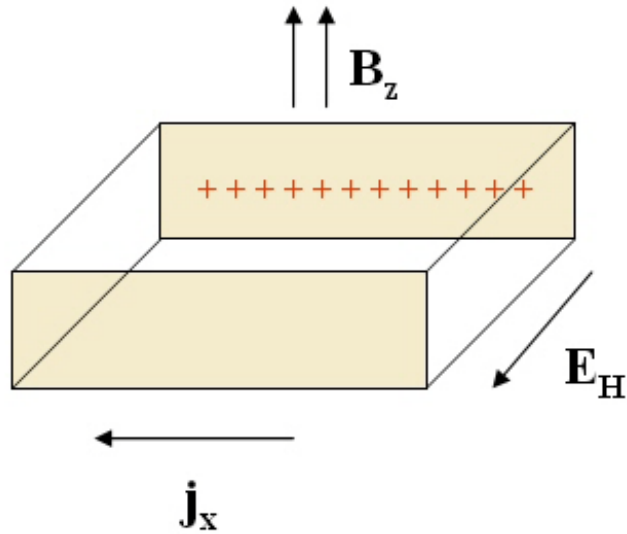
(*p*-type)

$$cq p \mu_h \frac{1}{pqc} = \mu_h$$

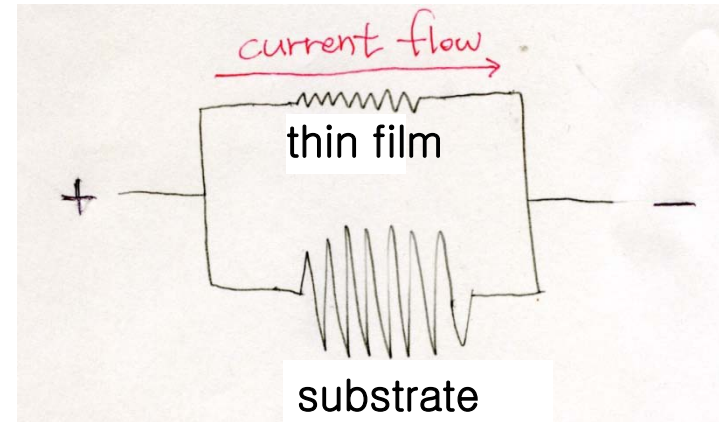
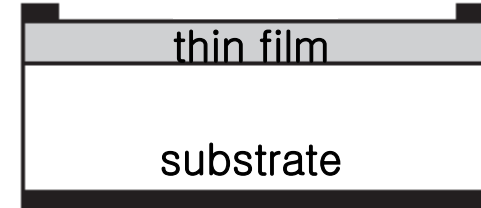
Hall mobility = Major carrier mobility

at high doping concentration

Hall Measurement for Thin Film



$$\mu_H = c\sigma R_H = c\sigma \frac{E_H}{j_x B_z}$$

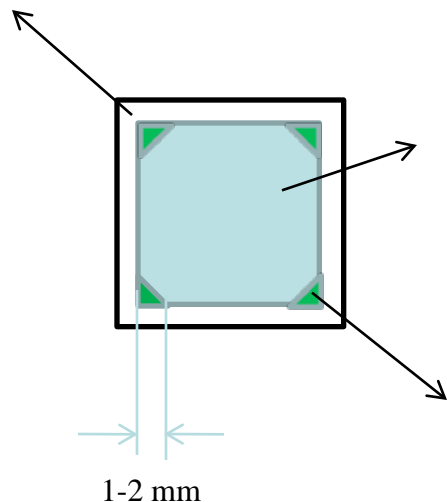


Highly Resistive Substrate

→ accurate Hall measurement of thin-film

Hall Measurement (반도체공동연구소)

기판 : 한 변의 길이는 2-2.1 cm

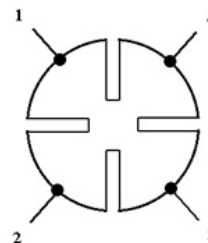


박막 :
한 변의 길이는 약 1.8 cm

metal contact

1-2 mm

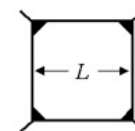
Cloverleaf



(a)

Preferred

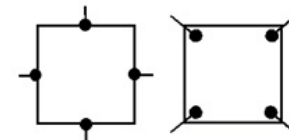
Square or
rectangle:
contacts at
the corners



(b)

Acceptable

Square or rectangle:
contacts at the edges
or inside the
perimeter



(c)

Not Recommended

<http://www.nist.gov/eel/semiconductor/hall.cfm> Figure 4

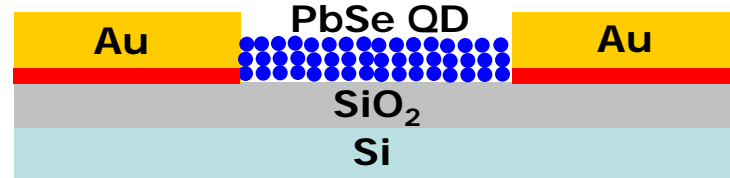
위의 schematic figure와 같이 박막의 네 귀퉁이에 metal contact 붙여 Hall measurement를 측정하려 가면 됩니다. Metal contact으로는 silver나 indium을 쓰는데 저의 경우(Al-doped ZnO 경우)에는 indium을 사용했을 시에 측정이 더 잘되었습니다.

오른쪽 그림의 (b)와 같이 삼각형 모양의 metal contact을 정확히 귀퉁이에 맞도록 붙이는 것이 가장 좋겠지만 손으로 붙이는 과정에서 현실적으로 정확히 그림과 같이 붙이기는 어려울 것입니다. 최소한 그림 (c)의 오른쪽 그림 처럼 metal contact이 박막 안쪽으로 들어가지는 않게 하는 것이 좋을 것 같습니다.

Metal contact의 크기는 사람 눈으로 보일 정도의 크기가 되는 선에서 되도록 작게 (현실적으로 위의 schematic figure와 같이 한 변의 길이가 1-2 mm 정도 되는 것이 한계일 것 같습니다.) 붙이는 것이 좋을 것입니다.

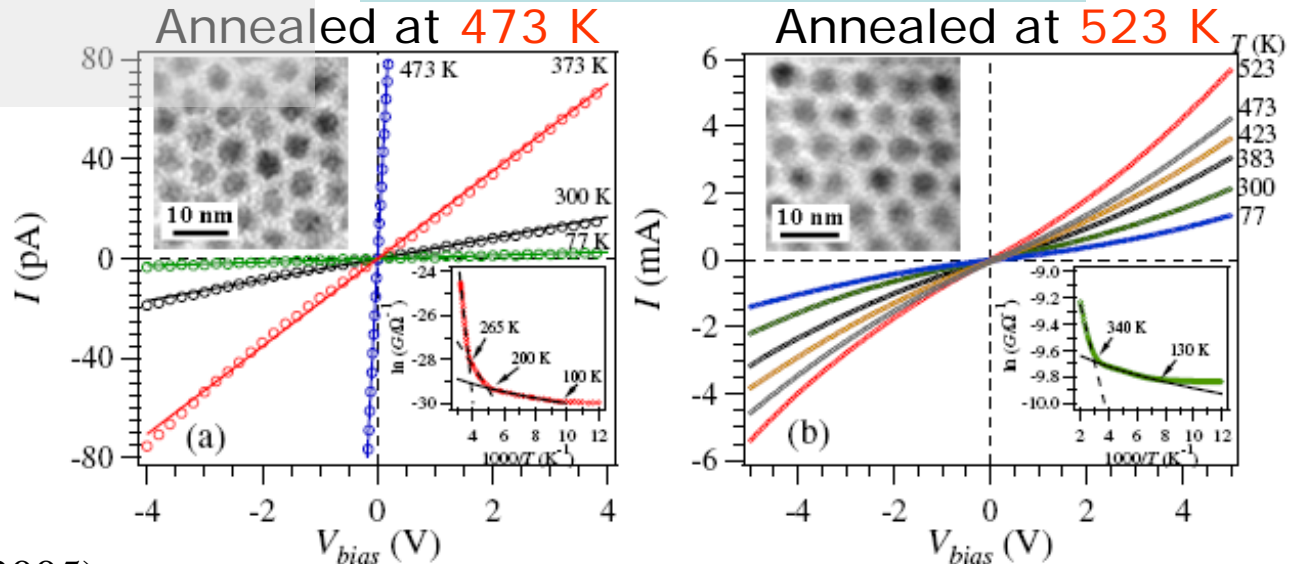
Coulomb Blockade and Hopping Conduction in PbSe Quantum Dots

Sample Preparation: Average size (PbSe nanoparticles) ~ 5.5 nm ($\sigma < 5.5\%$)
 Capped with oleic acid (~ 1 nm)
 Three-monolayers thick



Annealing: Tuning the distance between QDs

Tunable Quantum Dots



Phys. Rev. Lett. **95**, 156801 (2005).

입자간 간격 멀때 --> **Coulomb Blockade**

입자간 간격 중간 정도 --> **Electronic Hopping**

입자간 간격 가까울 때 --> **Quantum Tunneling**

* **Coulomb blockade** 양자점에서의 전자의 capacity는 온도에 의해 fluctuations이 있음. 그 fluctuation이 single electron 이하가 되려면 온도를 낮추거나 양자점이 아주 작아야 함. Si의 경우 10 nm 가 전자 1개의 fluctuation에 해당하고, 안정적으로 전자를 갖고 있으려면 1 nm 가량이 되어야 함. 그렇게 전자가 1-2개 order로 control이 될 경우 양자점에 1개의 전자가 들어가 있으면 coulomb repulsion 때문에 다음 전자가 들어 가는데 더 많은 에너지가 필요하게 되는 현상을 Coulomb blockade 현상이라고 함. 본 논문은 5 nm 정도 PbSe 나노입자가 상온에서 Coulomb blockade 현상을 보이고 있음.